Clinical Neurophysiology 174 (2025) 151–159

Contents lists available at ScienceDirect

Clinical Neurophysiology

journal homepage: www.elsevier.com/locate/clinph

Identification of the epileptogenic zone using phase–amplitude coupling on ictal stereoelectroencephalography

Tetsuya Ueda [a,b], Elodie Garnier [b], Damián Dellavale [b,c], Fabrice Bartolomei [b,d], Christian-George Bénar [b,*]

[a] Department of Neurosurgery, Epilepsy Center, Juntendo University, Tokyo, Japan
[b] Aix-Marseille Univ, INSERM, INS, Inst Neurosci Syst, Marseille, France
[c] Consejo Nacional de Investigaciones Científicas y Técnicas (CONICET), Centro Atómico Bariloche, R8402AGP, San Carlos de Bariloche, Río Negro, Argentina
[d] APHM, Timone Hospital, Epileptology and Cerebral Rhythmology, Marseille, France

ARTICLE INFO

Keywords:
harmonic PAC
Time locked index
Ictal analysis
Low voltage fast activity
Modulation index
Phase-amplitude coupling

ABSTRACT

Objective: Phase-Amplitude Coupling (PAC) has been proposed to characterize electrophysiological changes at seizure onset. However, PAC can arise from actual relations between oscillations at different frequencies (authentic PAC) or from harmonic/transient effects (spurious PAC). To assess the importance of these PAC mechanisms, we investigated the Modulation Index (MI) and Time Locked Index (TLI) between Epileptogenic Zone (EZ) and non-EZ channels during seizures.
Methods: We analyzed 34 patients with drug-resistant epilepsy who underwent stereoelectroencephalography (SEEG) implantation. SEEG data was classified into three periods: "preictal," "fast," and "rhythmic." The amplitude of ripple bands and the phase of three slow-wave bands were used for MI and TLI. The capacity of MI to detect the EZ was tested with precision and recall measures, summarized by the F1 score.
Results: The MI was significantly greater in EZ channels than that in non-EZ channels for all periods. The best F1 results were obtained for the "fast" period and spurious PAC. Both authentic and spurious PAC were present during all periods and bands.
Conclusions: Different PAC values could be observed during different seizure periods. Care should be taken when interpreting MI as a measure of authentic PAC.
Significance: MI and TLI can help the interpretation of ictal cross-frequency observations.

1. Introduction

Epilepsy surgery is the treatment of choice for patients with drug-resistant epilepsy. The success of surgery depends on the accurate delineation of the Epileptogenic Zone (EZ), which must be resected in order to obtain seizure freedom. To diagnose the EZ accurately, some patients require, following non-invasive recordings, an invasive procedure in the form of stereoelectroencephalography (SEEG). The interpretation of SEEG can be improved by signal processing, such as detection of interictal biomarkers like high-frequency oscillations (HFOs) (Bragin et al., 1999; Frauscher et al., 2017; Roehri and Bartolomei, 2019), ictal fast activity detection (Bartolomei et al, 2008), functional connectivity analysis (Bartolomei et al, 2002; Balatskaya et al 2020.), direct current (DC) shift (Ikeda et al., 1997), and entropy (Li et al., 2018; Bratu et al., 2024). However, no single marker has been recognized as surpassing all others (Roehri et al., 2018), and the exploration of new markers of the EZ remains an important challenge.

Cross-frequency coupling, particularly Phase-Amplitude Coupling (PAC), has been proposed as a new biomarker for the EZ. PAC describes a phenomenon whereby the amplitude of high frequency activity is modulated by the phase of low frequency activity. Since Weiss et al reported that PAC was more useful for the localization of an epileptic

Abbreviations: DC, direct current; EZ, epileptogenic zone; FDG-PET, fluorodeoxyglucose-positron emission tomography; FN, false negative; FP, false positive; FRs, fast ripples; HFO, high-frequency oscillation; LVFA, low-voltage fast activity; MI, modulation Index; MRI, magnetic resonance imaging; PAC, phase-amplitude coupling; PR, precision and recall; SEEG, stereoelectroencephalography; TLI, time locked index; TN, true negative; TP, true positive.

* Corresponding author at: Institut de Neurosciences des Systèmes (INS, UMR1106), Aix Marseille Université, INSERM, Marseille, France.
E-mail addresses: tueda@juntendo.ac.jp (T. Ueda), e.garnier30@gmail.com (E. Garnier), ddellavale@comahue-conicet.gob.ar (D. Dellavale), fabrice.bartolomei@ap-hm.fr (F. Bartolomei), christian.benar@univ-amu.fr (C.-G. Bénar).

https://doi.org/10.1016/j.clinph.2025.03.029
Accepted 20 March 2025
Available online 27 March 2025
1388-2457/© 2025 The Authors. Published by Elsevier B.V. on behalf of International Federation of Clinical Neurophysiology. This is an open access article under the CC BY license (http://creativecommons.org/licenses/by/4.0/).

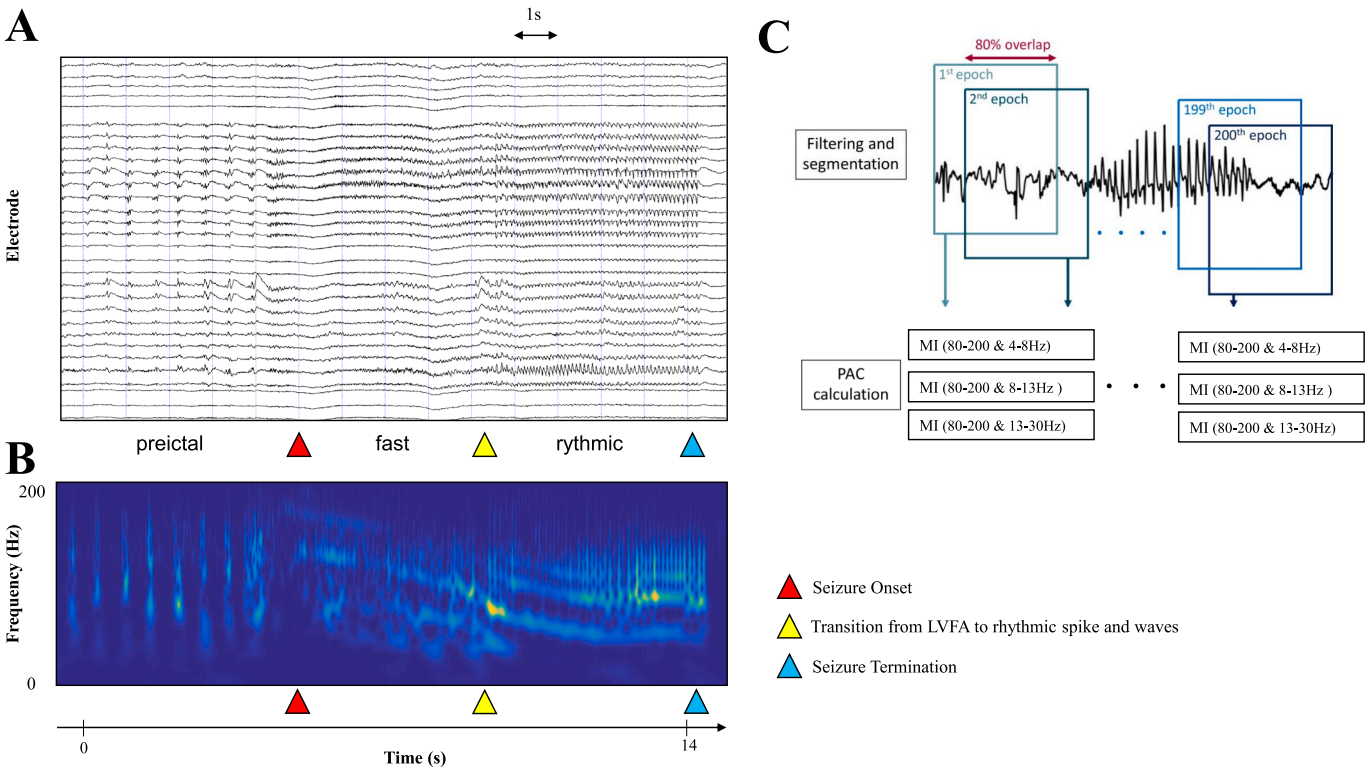


Fig. 1. Schematic view of analysis pipeline (A) A representative seizure (Case #11) is shown from 5 s before seizure onset to termination on stereo-electroencephalography. (B) Time-frequency analysis of the same time period. The entire paraictal time window is divided into three periods. Seizure onset is indicated by a red arrowhead. The yellow arrowhead indicates the transition from a low-voltage fast activity to rhythmic spikes and waves. Seizure termination is indicated with a blue arrowhead. (C) Phase-Amplitude Coupling (PAC) analysis scheme. The upper subfigure shows segmentation using a 1-epoch time window with 80% overlap. The lower subfigure represents the PAC analysis results for the three-band combinations. The modulation index (MI) was obtained for each combination and each period Abbreviations: LVFA, low-voltage fast activity; MI, modulation index; PAC, phase-amplitude coupling. (For interpretation of the references to colour in this figure legend, the reader is referred to the web version of this article.)

Table 1
Patient statistics.

	n = 34
Sex (M:F)	15:19
Seizure	Range 1–5, mean 2.8, SD 0.9
Age at seizure onset (years)	Range 1–40, mean 12.1, SD 9.5
Age at SEEG (years)	Range 5–56, mean 25.7, SD 13.1
Electrode channels	Range 34–165, mean 3228, SD 28.3
EZ	Range 4–48, mean 611, SD 10.2
non-EZ	Range 23–141, mean 2617, SD 27.7
MRI	
Positive	29 (85 %)
Negative	5 (15 %)
Seizure etiology	
Hippocampal sclerosis	9 (26 %)
Focal cortical dysplasia	7 (21 %)
Tumor	6 (17 %)
Post-stroke	3 (9 %)
Post-surgical scar	2 (6 %)
Tuberous sclerosis	1 (3 %)
Encephalitis	1 (3 %)
Trauma	1 (3 %)
Unknown	4 (12 %)
Seizure semiology	
Temporal	15 (44 %)
Frontal	7 (21 %)
Temporo-frontal	4 (12 %)
Insular	3 (9 %)
Parietal	2 (6 %)
Temporo-occipital	1 (3 %)
Occipital	1 (3 %)
Central	1 (3 %)

Abbreviations: EZ, epileptogenic zone; SEEG, stereoelectroencephalography; MRI, magnetic resonance imaging.

focus than high γ amplitude alone (Weiss et al., 2013), several couplings between δ (Nariai et al., 2011; Iimura et al., 2018), θ (Ibrahim et al., 2014; Hashimoto et al., 2021), α (Ibrahim et al., 2014), and β (Edakawa et al., 2016) phases and HFO analysis have recently been the focus of attention as potential biomarkers for EZ during interictal period. Furthermore, the ictal period was reported to disclose prominent features in terms of cross-frequency interactions. (Motoi et al., 2018). However, it is to be noted that seizure onset and termination may have widely different patterns on SEEG (Lagarde et al., 2019; et al., Shokooh et al., 2021), which could impact cross-frequency analysis. The most frequent patterns, which would be important to investigate, involve low-voltage fast activity (LVFA) pattern at seizure onset (Lagarde et al., 2019), and the rhythmic spike-and-wave pattern at termination (Evangelista et al., 2015, Shokooh et al., 2021).

In a previous study, we reported that PAC changes during the ictal phase on intracranial EEG (Ueda et al., 2023) and distinguished between the EZ channels and non-EZ channels depending on combinations of slow waves and HFOs. However, it is important to note that increased measures of PAC can arise from very different mechanisms. The first mechanism, sought by the measure, is the actual occurrence of bursts of high frequency oscillatory activity during specific phases of low frequency oscillation This is referred to here as 'authentic PAC' (Jurkiewicz et al., 2021). The second is the presence of transients (epileptic spikes) or harmonic frequencies, which can both produce trivial relationships between the phase at low frequencies and the energy at high frequencies (Supp. Fig. 1) (Bénar et al., 2010). This will be referred to here as 'spurious PAC', which is remarked as false PAC in previous study (Jurkiewicz et al., 2021).

The Time Locked Index (TLI) has been introduced recently in order to measure harmonic PAC, which can occur in the presence of a non-

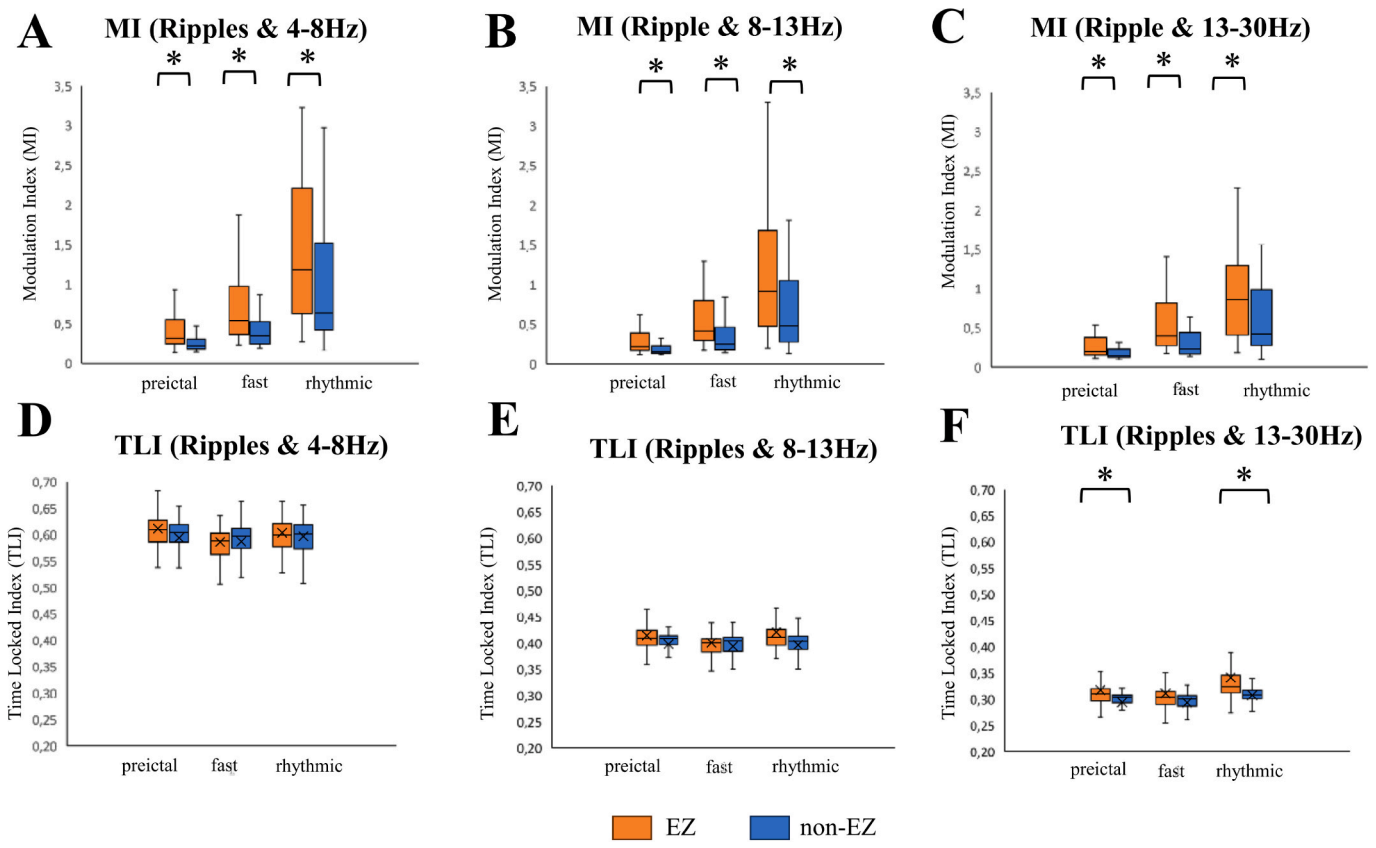


Fig. 2. Modulation index and time locked index for the three periods Modulation indices (MIs) between ripples and 4–8 Hz (A), 8–13 Hz (B), and 13–30 Hz (C) were analyzed for the three periods (preictal, fast and rhythmic). The MI was significantly greater in the epileptogenic zone (EZ) group than that in the non-EZ group in all periods ($p < 0.05$). The time locked index (TLI) for each period was also compared between the EZ and non-EZ groups (D–F). The TLIs (ripples and 13–30 Hz) in the preictal and rhythmic periods were significantly greater in the EZ group than that in the non-EZ group ($p < 0.05$) (F). No significant differences between the EZ and non-EZ groups were observed during the fast period. Abbreviations: EZ, epileptogenic zone; MI, modulation index; TLI, time locked index.

sinusoidal periodic component (Dellavale et al., 2020). Dellavale and colleagues reported that harmonic and non-harmonic PAC coexist in the EZ during the ictal phase, and the harmonicity analysis (e.g., via the TLI measure) could play a relevant role in the interpretation of the ictal mechanisms. Importantly, bursts of epileptic spikes, which bear energy across all frequencies, should also lead to high values of PAC and TLI (Supp. Fig. 1). The evidence discussed above suggest that authentic and spurious PAC emerge from essentially different mechanisms with an impact in their performance to identify the EZ. However, most studies devoted to the analysis of PAC as a biomarker for EZ identification in general overlook the harmonicity properties of the observed PAC patterns, which might lead to incomplete or misleading interpretations of the results. In addition, initial results on classification of PAC as spurious or authentic did not consider the different seizure sections separately, even though dynamic aspects have been shown to be important (Ueda et al 2023).

The goal of the present study was thus to assess the relative importance of authentic and spurious PAC in defining the EZ in SEEG across the different seizure periods. For this, we analyzed the SEEG recordings of patients with seizure-free outcome after epilepsy surgery, from seconds before seizure onset to seizure termination. Since PAC changes depending on the seizure phase (Ueda et al., 2023), SEEG data during seizures were classified into three periods: “preictal”, “fast” and “rhythmic”. We investigated the PAC and TLI between the EZ channels and non-EZ channels during each period.

2. Methods

2.1. Participants

We retrospectively analyzed 34 patients who underwent SEEG investigation in our department (Epileptology and Cerebral Rythmology, Timone Hospital, Assistance Publique Hôpitaux de Marseille, France).

Before SEEG implantation, all patients underwent scalp EEG, brain magnetic resonance imaging (MRI), fluorodeoxyglucose-positron emission tomography (FDG-PET), medical history, and neuropsychological testing. Imaging studies, including MRI and FDG-PET, were evaluated by experienced neurologists and neurosurgeons. All patients in this study required SEEG to define the EZ according to French guidelines (Isnard et al, 2018). The placement of SEEG electrodes was decided based on non-invasive information during a multidisciplinary meeting. The reference for SEEG recording was set in a region that was deemed as ‘silent’, typically using a contact within the skull.

The histological diagnosis complied with the current guidelines of the International League Against Epilepsy and the World Health Organization (Blümcke et al., 2013; Louis et al., 2016). Surgical outcomes were assessed using the Engel classification during the postoperative follow up period (Engel, 1993). In this study, patients were selected based on the Engel classification I outcome, in order to have a ‘ground truth’ for EZ delineation.

2.2. Seizure analysis

SEEG exploration was carried out during long-term video-EEG

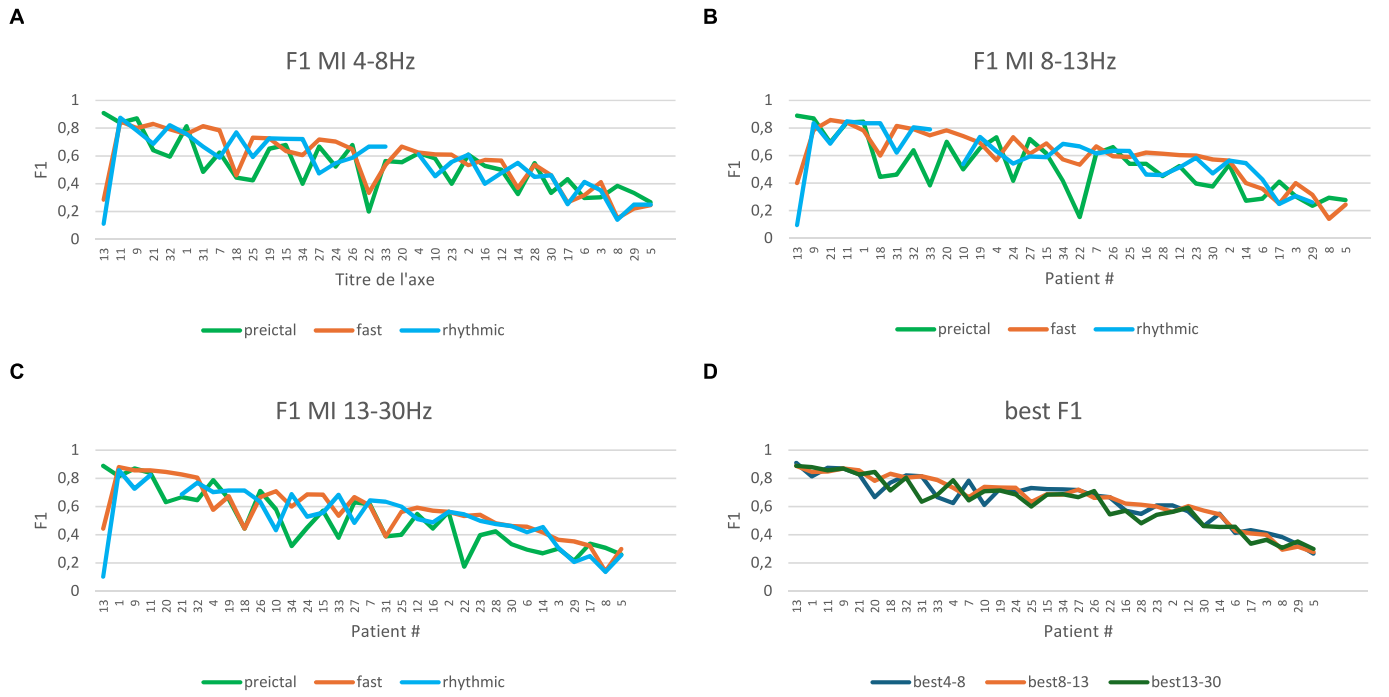


Fig. 3. F1 score for the modulation index for the three periods The F1 scores were organized and ranked at each band and each period(A–C). No significant differences were identified between bands and periods (after false discovery rate correction for multiple comparison). The F1 scores among each period were ordered from highest to lowest (D). A proportion of 58.8% of the patients had their maximum score across all bands and periods above 0.7. Abbreviations: MI, modulation index.

Table 2
Precision and recall.

	Precision	Recall	F1 score
MI (Ripple & 4–8 Hz) Preictal period	0.773	0.514	0.556
MI (Ripple & 4–8 Hz) Fast period	0.72	0.531	0.558
MI (Ripple & 4–8 Hz) Rhythmic period	0.714	0.53	0.526
MI (Ripple & 8–13 Hz) Preictal period	0.756	0.524	0.563
MI (Ripple & 8–13 Hz) Fast period	0.727	0.555	0.579
MI (Ripple & 8–13 Hz) Rhythmic period	0.743	0.513	0.519
MI (Ripple & 13–30 Hz) Preictal period	0.777	0.487	0.544
MI (Ripple & 13–30 Hz) Fast period	0.716	0.604	0.584
MI (Ripple & 13–30 Hz) Rhythmic period	0.73	0.491	0.504

Abbreviations: MI, modulation index.

monitoring. Recordings were performed using intracerebral multiple contact electrodes (10–15 contacts; length, 2 mm; diameter, 0.8 mm; 1.5 mm apart; for details see previous report) (Bartolomei et al., 2008). In our study, we analyzed SEEG data from 10 s before seizure onset to seizure termination using the AnyWave in-house software (Colombet et al., 2015, available at meg.univ-amu.fr). Electrodes with artifacts were excluded from the analysis. The SEEG was recorded at a sampling rate of 512 Hz or 1024 Hz depending on the recording period. All seizure onsets were marked visually (T.U.). Seizure onset was defined by the occurrence of LVFA, often preceded by interictal-ictal transitional changes (preictal spiking, DC shift, burst of polyspikes) (Lagarde et al., 2019). Seizure termination was defined as the time point when the rhythmic discharge ended (Ueda et al., 2023).

Ictal SEEG data was classified into three periods according to changes in the SEEG signal (Fig. 1). The first period was the "preictal period," corresponding to 10 s before seizure onset (before the red arrowhead in Fig. 1A). The second period was the "fast period," with only an LVFA component (between the red and yellow arrowheads in Fig. 1A). The third period was the "rhythmic period," corresponding to continuous rhythmic spikes and waves lasting until seizure termination (between the yellow and blue arrowheads in Fig. 1A, B).

The Epileptogenic Zone (EZ) was defined based on visual analysis of SEEG data (Bartolomei et al 2018) with the help of a quantitative method, the epileptogenicity index (Bartolomei et al 2008). We followed the French guidelines (Isnard et al 2018) on the definition of the epileptogenic zone, i.e., as the brain regions primarily involved in seizure genesis.

2.3. Phase amplitude coupling based on modulation index

The Modulation Index (MI) method was introduced to quantify PAC (Canolty et al., 2006; Özkurt and Schnitzler, 2011). In this study, MI was calculated on the monopolar montage using the Phase-Amplitude Coupling Toolbox in MATLAB (MathWorks, Natick, MA, USA) (Miyakoshi et al., 2013). In theory, the MI is greater when appearance of HFO is coupled with the phase of slow waves (Nonoda et al., 2016). Monopolar montage is often used for PAC analysis because it allows for the examination of specific brain regions' phase and amplitude relationships accurately. Additionally, monopolar montage provides a broad coverage of brain activity, making it well-suited for PAC analysis, which often requires capturing activity from multiple brain regions simultaneously.

MI analysis was carried out from 10 s before seizure onset to seizure termination according to the same methodology as that in our previous study (Ueda et al., 2023). A sliding window technique with overlapping was employed for MI calculation to reduce the effect of information leakage across windows. Each time window lasted 1 s long and an 80 % overlap was applied. Then, MI was calculated at each phase, which reflected the degree of coupling between ripple amplitude (80–200 Hz) and three different frequency band activities (4–8 Hz, 8–13 Hz, and 13–30 Hz) (Fig. 1C).

2.4. Performance of classification based on precision and recall curve

Precision and recall (PR) curves quantify the performance of a classification model. The PR curve is more suitable than the receiver

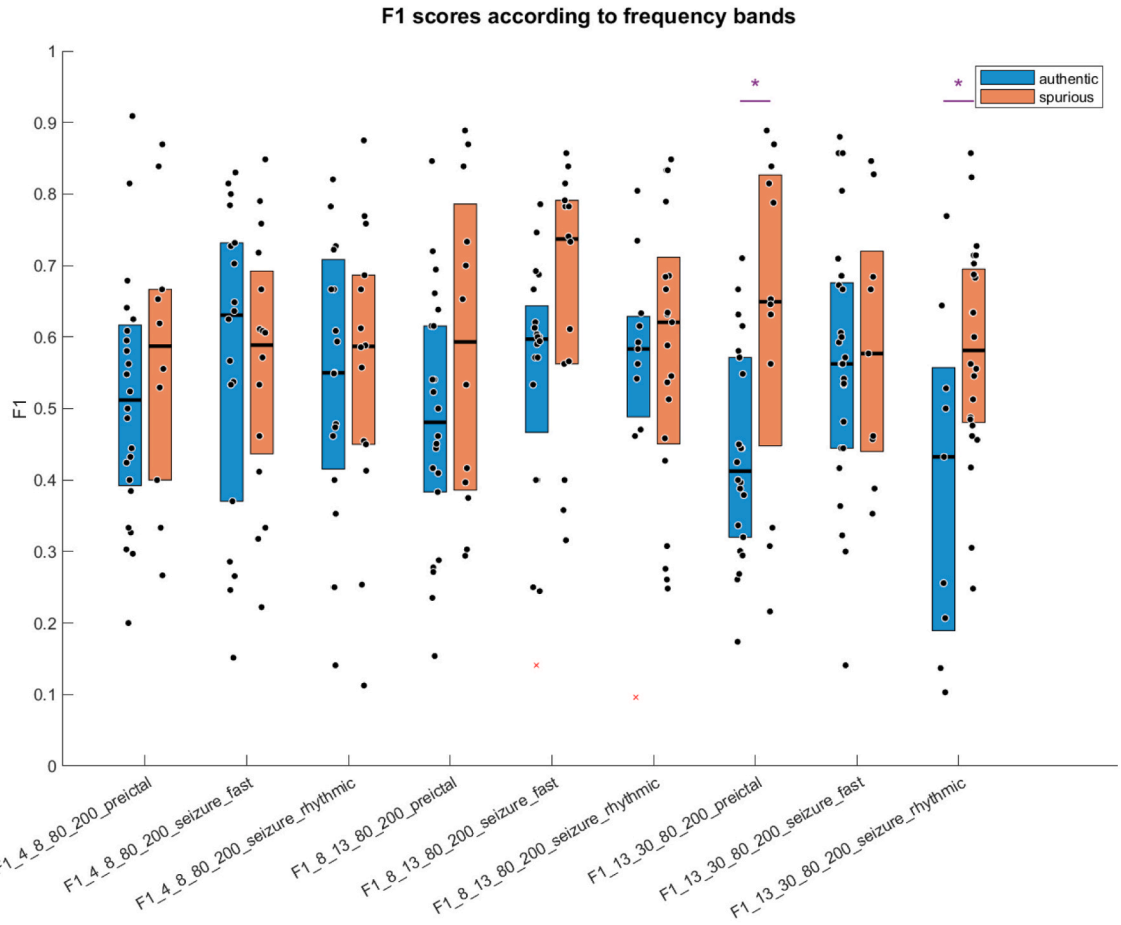


Fig. 4. F1 scores according to the different frequency bands and seizure periods. The best median F1 for the authentic PAC was 63 % (4–8 Hz band in the fast period), and the best for the spurious PAC was 73 % (8–13 Hz band in the fast period). There was a significantly higher F1 score for the spurious mechanisms in the 13–30 Hz band for the preictal period and for 13–80 Hz band in the rhythmic period ($p < 0.05$, indicated by a star).

operating characteristic curve, based on sensitivity and specificity, for imbalanced datasets. In this study, the level of imbalance was large, given that the data had many more non-EZ channels than EZ channels, which led to high values of specificity, even for a high level of false detections, compared with the number of true detections. The confusion matrix included four values: true positives (TP), the amount of EZs correctly classified as EZs; true negatives (TN), the amount of non-EZs correctly classified as non-EZs; false positives (FP), the amount of non-EZs misclassified as EZs; and false negatives (FN), the amount of EZs misclassified as non-EZs. In order to evaluate the performance of the model, Precision, Recall, and F1 score were used. Definitions are provided in formulae 3–5. Precision measured, among all detected EZ electrodes, how many were actual EZ electrodes (positive predictive value). Recall measured how many EZ electrodes were successfully detected (i.e., sensitivity). The F1 score was the harmonic mean of precision and recall.

$$\text{Precision} = \frac{\text{TP}}{\text{TP} + \text{FP}} \tag{1}$$

$$\text{Recall} = \frac{\text{TP}}{\text{TP} + \text{FN}} \tag{2}$$

$$\text{F1 score} = \frac{2\text{TP}}{2\text{TP} + \text{FP} + \text{FN}} \tag{3}$$

2.5. Time-locked index for quantifying spurious PAC

The Time-Locked Index (TLI) was introduced to quantify the extent to which high frequency activity phase-locked to low frequency activity (Dellavale et al., 2020). Such locking occurs in the presence of non-sinusoidal activity, which has harmonics, or in the presence of bursts of spikes. We used the procedure presented in the study by Dellavale et al. (2020) in order to calculate TLI and use it to discriminate between authentic and spurious PAC. In summary, the peaks in the low-pass filtered data were detected and used to compute a time-locked average of the signals. In the case of non-sinusoidal oscillations, the signals filtered in the high-frequency band were phase-locked to the low-pass filtered signals, thus resulting in an average with high amplitude. Filtering artifacts attributed to epileptic spikes (Bénar et al., 2010) also result in a significant time-locked average, with maximal value if they occur in a rhythmic burst at a low frequency of interest (Supp. Fig. 1). Whether an MI value arises from spurious PAC may be detected by performing regression between MI and TLI values across contacts within each patient (Dellavale et al., 2020). A significant correlation between the two sets of values suggest that PAC is of a spurious nature.

2.6. Statistical analysis

Statistical analysis was performed using the EZR software which is based on R and R commander (Kanda, 2013). First, a Mann-Whitney *U* test was performed to compare the differences between the EZ group and non-EZ group in each period using PAC and TLI. Second, to evaluate

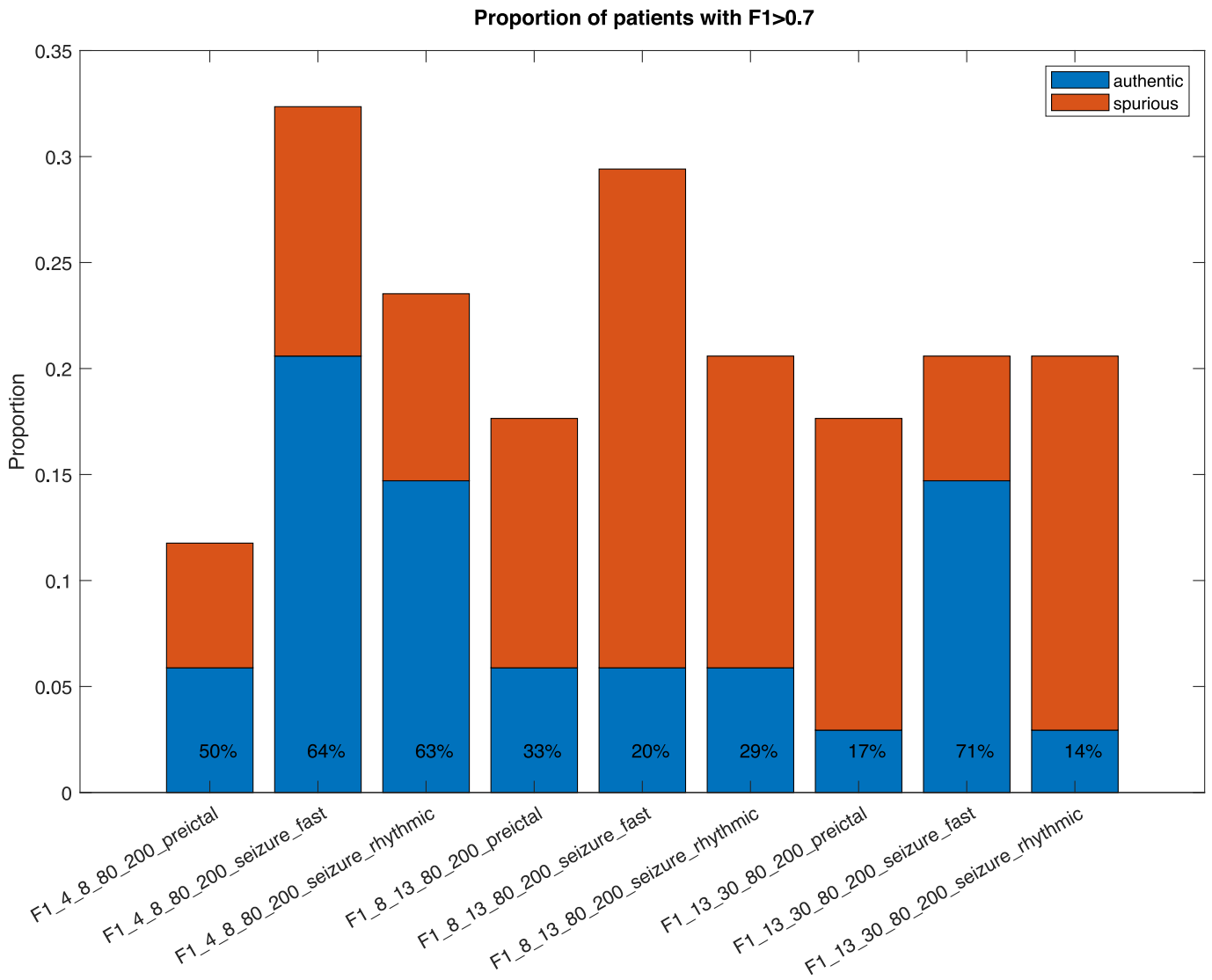


Fig. 5. Authentic versus spurious phase-amplitude coupling The height of each bar represents for each band and period the proportion of patients with an F1 score above 0.7. Within each bar, the proportion of authentic Phase-Amplitude Coupling (PAC) is shown. The highest proportion of authentic PAC was 71 % for the coupling between ripples and 13–30 Hz in the rhythmic period. The smallest proportion was 14 % for the coupling between ripples and 13–30 Hz in the rhythmic period.

whether PAC was useful for detecting the EZ, the F1 score was computed for each seizure period and each frequency band, and a Wilcoxon with Bonferroni correction was performed for 3 comparisons. Statistical significance was set at a false discovery rate p-value of 0.05.

2.7. E*thical approval

The study was approved by the local ethical committee of AP-HM. All procedures were in accordance with the ethical standards of the institutional research committee and with the 1964 Helsinki declarations and its later amendments or comparable standards.

3. RESULTS

3.1. Patient profile

In total, data of 34 patients (19 female and 15 male) were analyzed for this study. The mean number of seizures per patient was 2.8 (range 1–15, SD 0.9), with a total of 96 seizures analyzed. The mean age at epilepsy onset was 12.1 years (range 1–40, SD 9.5), the mean age at SEEG was 25.7 years (range 5–56, SD 13.1), and the mean epilepsy duration before SEEG was 13.6 years (range 3–56, SD 10.5). A total of 3228 channels were analyzed in these patients, of which 611 channels were in the EZ (mean of 17.9 channels per patient, range 4–48, SD 0.2), and 2617 channels were in non-EZ (mean of 76.9 channels per patient, range 23–141, SD 27.7). The duration of the preictal period was fixed to 10 s, the mean duration of the fast period was 17.1 s (range 2.2 s-38.3 s, SD 7.5), and the mean duration of the rhythmic period was 56.1 s (range 10.5 s-128.5 s, SD 15.6). Patient characteristics are provided in Table 1.

3.2. Phase amplitude coupling based on modulation index

Examples of time frequency and MI computation are shown in Supplementary Fig. 2. The MI for each combination of frequency bands was compared between the EZ and non-EZ groups in each seizure phase (Fig. 2A–C). For all phases and couplings between ripples band and slow frequency band, MIs were significantly greater in the EZ group than those in the non-EZ group (Mann-Whitney U test, $p < 0.05$). In the EZ group, the MI increased gradually from seizure onset to seizure termination for each combination of slow waves and HFO.

For each patient, we computed the F1 score to quantify the capacity of the MI to serve as a marker of the EZ for each seizure period and each frequency band (Fig. 3). No major difference was identified between the frequency bands. Regarding the MI (ripples and 8–13 Hz) and MI (ripples and 13–30 Hz), the fast period generally yielded better results than the preictal period (paired Wilcoxon, $p < 0.05$ with Bonferroni correction for 3 comparisons) (Fig. 3A–C). The mean F1 score for the MI (ripples and 13–30 Hz) was better in the fast period than that in any other MI (mean precision = 0.716, recall = 0.604, and F1 score = 0.584) (Table 2). The best score across all periods is presented in Fig. 3D. For MI (ripples and 4–8 Hz) and MI (ripples and 8–13 Hz), 15 patients out of 34 had F1 scores of > 0.7. For MI (ripples and 13–30 Hz), 14 patients (41.1 %) had F1 scores of > 0.7. Across all bands, 58.8 % of the patients (20 out of 34) had best F1 scores of > 0.7.

3.3. Time-locked index for quantifying spurious PAC

The TLI permits to verify for each patient whether PAC arises from authentic interactions between processes at different frequencies or from spurious (harmonics-related) activity. Examples of time frequency and TLI computation are shown in Supplementary Fig. 2. To verify the presence of spurious PAC, the TLIs were analyzed between the EZ and non-EZ groups at each phase (Fig. 2D–F). The TLI (ripples and 13–30 Hz) was significantly greater in the EZ group than that in the non-EZ group during the preictal and rhythmic periods (Mann-Whitney *U* test, $p < 0.05$). In the fast period, no interaction was detected between the EZ and non-EZ groups in the TLI (ripples and 13–30 Hz). The TLI (ripples and 4–8 Hz) and TLI (ripples and 8–13 Hz) exhibited no significant differences at any period between the EZ and non-EZ groups.

For each frequency band and period, we compared across patients the F1 score for detection of EZ between authentic and spurious cases (Fig. 4). Both mechanisms were present, with a significantly higher F1 score for the spurious mechanisms in the 13–30 Hz band for the preictal period and for 13–80 Hz band in the rhythmic period. The best median F1 for the authentic PAC was 63 %, obtained for the 4–8 Hz band in the fast period. The best median F1 for the spurious PAC was 73 %, obtained for the 8–13 Hz band, for the fast period.

Then, we computed the proportion of patients with an F1 score of > 0.7, indicating that MI was a good marker of the EZ (Fig. 5). The lowest proportion (12 %) was obtained in the preictal period and the 4–8 Hz band. The highest proportion (32 %) was obtained in the fast period and 4–8 Hz band, followed by the fast period and 8–13 Hz band (29 %). Among these patients, we measured the proportion of authentic and spurious PAC, as indicated by a significant regression of TLI on PAC. A high variability was identified between periods and bands. The smallest proportions of authentic PAC were 14 %, in the coupling with 13–30 Hz band in the rhythmic period, and 17 %, in the coupling between ripples and 13–30 Hz band, and 14 % in the preictal and rhythmic periods. The highest values were observed for 13–30 Hz in the rhythmic period (71 %), 4–8 Hz in the fast period (64 %), 4–8 Hz in the rhythmic period.

4. Discussion

This study investigated 96 seizures in 34 patients with drug-resistant epilepsy who had undergone SEEG electrodes implantation. Phase-amplitude coupling (PAC) was measured from 10 s before seizure onset until seizure termination, in order to assess the capacity of this metric to serve as a marker of the EZ. SEEG data was classified into three periods, “preictal,” “fast,” and “rhythmic”, based on raw SEEG data. PAC was quantified with the Modulation index (MI), and Time-Locked index was used in order to distinguish authentic and spurious PAC. To our knowledge, this report is the first to document the two different PAC mechanisms across different seizure periods.

Ictal analysis is considered to be the key period for defining the EZ, considered to be more effective than interictal analysis (Motoi et al., 2018) (even though this varies according to epilepsy type (Bartolomei et al., 2016)). However, seizure outcomes after focal resection have not improved significantly, despite the introduction of computational methods (Jacobs et al., 2018). This may be attributed to the difficulty in finding reliable biomarkers across variable etiologies and observed patterns (Lagarde et al., 2019).

An interesting venue is to consider the interaction between activities in different frequency bands. Oscillations in themselves have been shown to be important markers of epilepsy, either in High frequency band or in the gamma band (Thomas et al., 2023, Jmail et al., 2016). As oscillations arise in periods of high excitibility, it is natural to investigate the actual coupling between low frequency activity (which modulates excitability) and oscillations. Such coupling has been shown to be a ubiquitous mechanism in physiological activity. It has also been shown to arise during epileptic discharges (Ueda et al., 2023), making it is a candidate marker for delineating the epileptogenic zone.

In this study, after classifying the ictal SEEG into three periods, the PAC, quantified by MI, was found to be greater in the EZ group than that in the non-EZ group (Fig. 2). The highest values of PAC were observed in the rhythmic period, but the best discrimination between EZ and non-EZ was obtained in the preictal and fast periods. The effective results in the fast period were particularly noteworthy, as this is usually a period of desynchronization (Wendling et al., 2003) and corresponds with inhibitory processes (Elahian et al., 2018, Grinenko et al., 2018). These results could be ascribed to a mixture of patterns in the fast period, which include variables apart from the actual low frequency fast discharges (Lagarde et al., 2019). The fact that there is worse discrimination (Fig. 2,3) despite high MI values could arise in part from the fact that high PAC measures can result from bursts of spikes (Jurkiewicz et al., 2021, Dellavale et al., 2020) (Supp. Fig. 1), which may be more independent of the epileptogenic nature of a region, compared with pure propagation.

From a pure ‘detection’ point of view (i.e., as a marker of the epileptogenic zone), good performance (F1 score of > 0.7) was observed only in a proportion of patients, ranging from 12 % to 32 %. The best results were observed in the fast period and the 4–8 Hz band, suggesting that the PAC marker should be used in conjunction with other markers. Other features of PAC could also be considered (Li et al., 2023).

A large proportion of the MI findings with good performance could be attributed to ‘spurious’ PAC, which may not correspond to an actual link between oscillatory processes but may correspond to a trivial time–frequency structure of the bursts of epileptic spikes (Bénar et al., 2009, Jmail et al., 2017). This confirms the fact that PAC measures should be interpreted with caution. Still, they could be in some cases interesting features to consider, as spikes that are more ‘spiky’ could be a marker of the EZ (Köksal-Ersöz et al., 2022) and lead to higher (even though spurious) PAC measures. Further investigations are required on spike features within seizures.

In line with the above discussion, our results suggest that non-harmonic Theta-Ripple and Alpha-Ripple PAC observed during the fast period could be used to complement other clinically relevant EZ biomarkers like the phase-locked high gamma (PLHG, Weiss et al., 2013). Specifically, retrospective studies based on the postoperative surgical outcome of epilepsy surgery patients, have shown the clinical relevance of ictal PAC between slow (1–25 Hz) and Ripple (80–200 Hz) bands, as assessed by the PLHG measure, as a biomarker to improve the spatial delineation of resection boundaries associated to the ictal core from EEG recordings with macroelectrodes (Weiss et al., 2013). However, the PLHG measure is susceptible to the harmonics of the slow rhythms as a confounding factor since slow non sinusoidal rhythms (e.g. in the theta to beta bands) can produce prominent harmonically related spectral components, which extend inside the ripple band. In this regard, our results point out that non-harmonic Theta-Ripple PAC observed during the fast period is a biomarker of EZ outperforming, in terms of precision and recall, other PAC measures not including the segregation in periods or the harmonicity analysis. As a consequence, our results constitute a step forward in the process of improving the EZ biomarkers based on

PAC for clinical use.

4.1. Limitations

There are some limitations of this study. Firstly, our analysis window was one second which is insufficient for evaluating the phase of the infraslow wave (<1Hz) and δ band (1–4 Hz). It has however been reported that the DC shift composed of very slow frequency is related to epileptic seizures (Ikeda et al., 1997) and PAC between δ and HFO is useful for detecting EZ. Additional work is needed to confirm how PAC and TLI behave at frequencies less than 4 Hz, keeping in mind that several windows are necessary for computing robustly our measures – one would need sustained phenomenon across a long time period. Moreover, and about DC shift, this later has been shown as another marker of the epileptogenic zone, with different topography thatn the fast activity (Thompson et al., 2016); meaning that the actual relationship between PAC and slow activity should be investigated on its own.

Secondly, the study did not analyze the PAC and TLI between slow waves and fast ripples (FRs) that is oscillations above 200–300 Hz. However, FRs have been shown to be more specific than ripples for detecting the seizure onset zone on interictal EEG using HFO (Urrestarazu et al., 2006). To investigate FRs, one would need a sampling frequency of at least 2 kHz. Further studies are needed regarding FR on ictal EEG using TLI and MI.

Thirdly, we did not control for the exact location of the reference electrode, even though the processing was performed in a referential montage (in order to preserve low frequency, widespread activity), which can be sensitive to fluctuations from the reference channel. As mentioned in the methods section, the reference was set in a region deemed as 'silent' in order to limit these effects. Multivariate signal analysis such as Independent Component analysis could be applied to SEEG signals (Medina Villalon et al., 2024) in order to lower the impact of the reference channel (Madhu et al., 2012), and also to disentangle potential different generators of low frequency activities (López-Madrona et al., 2020).

5. Conclusions

In this study, for the first time, we presented MI and TLI results for each seizure period. PAC was greater in the EZ group than that in the non-EZ group during all periods. In particular, PAC (ripples and 13–30 Hz) can help identify the EZ in some cases, particularly in the fast period, suggesting that PAC can have clinical usefulness. The study also found that spurious PAC can be observed across all periods and bands, which emphasizes the importance of not over-interpreting the PAC measure. Further investigation of PAC as a complementary marker of the EZ among a series of other features will be useful. This could lead to a larger retrospective study with machine learning applied on a series of markers (with distinction between spurious and authentic PAC), and the output tested in a retrospective study where markers would be presented to the clinical staff during the presurgical evaluation phase. On a more fundamental point of view, the opportunity to distinguish between authentic and spurious PAC could shed light on ictal mechanisms.

Notation of prior abstract publication/presentation

None.

Author Contribution

Tetsuya Ueda: Contribution to data analysis and figure drafting. Wrote the first draft of the manuscript.

Elodie Garnier: Contribution to data analysis. Revising the manuscript.

Damián Dellavale: Contribution to data analysis. Revising the manuscript.

Fabrice Bartolomei: Conception and design of the project. Interpretation of results. Revising the manuscript.

Christian Bénar: Conception and design of the project. Design of data analysis scheme. Interpretation of results. Manuscript writing and revising.

All the authors have approved the final article.

Funding

This work was supported by Japan Science and Technology-Core Research for Evolutional Science and Technology (grant number JPMJCR20F1 to TU). EG was funded in part by the European Research Council under Galvani Project, ERC-SyG 2019, Grant Agreement No. 855109. DD was funded in part by ANR Neurosense ANR-18-CE19-0013.

Acknowledgements

The authors thank Romain Carron for the SEEG implantation that led to these clinical data. We would like to thank Editage (www.editage.com) for the English language editing.

Appendix A. Supplementary data

Supplementary data to this article can be found online at https://doi.org/10.1016/j.clinph.2025.03.029.

References

Balatskaya, A., Roehri, N., Lagarde, S., Pizzo, F., Medina, S., Wendling, F., et al., 2020. The "Connectivity Epileptogenicity Index " (cEI), a method for mapping the different seizure onset patterns in StereoElectroEncephalography recorded seizures. Clin Neurophysiol 131 (8), 1947–1955. https://doi.org/10.1016/j.clinph.2020.05.029.

Bartolomei, F., Nica, A., Valenti-Hirsch, M.P., Adam, C., Denuelle, M., 2018 Feb. Interpretation of SEEG recordings. Neurophysiol Clin. 48 (1), 53–57. https://doi.org/10.1016/j.neucli.2017.11.010 (Epub 2017 Dec 27 PMID: 29289423).

Bartolomei, F., Trébuchon, A., Bonini, F., Lambert, I., Gavaret, M., Woodman, M., Giusiano, B., Wendling, F., Bénar, C., 2016. What is the concordance between the seizure onset zone and the irritative zone? A SEEG quantified study. Clin Neurophysiol. 127 (2), 1157–1162. https://doi.org/10.1016/j.clinph.2015.10.029 (Epub 2015 Oct 19 PMID: 26520456).

Bartolomei, F., Wendling, F., Vignal, J., Chauvel, P., Liégeois-Chauvel, C., 2002. Neural networks underlying epileptic humming. Epilepsia 43 (9), 1001–1012. https://doi.org/10.1046/j.1528-1157.2002.48501.x.

Bartolomei, F., Chauvel, P., Wendling, F., 2008. Epileptogenicity of brain structures in human temporal lobe epilepsy: a quantified study from intracerebral EEG. Brain 131 (7), 1818–1830. https://doi.org/10.1093/brain/awn111.

Bénar, C.G., Chauvière, L., Bartolomei, F., Wendling, F., 2010. Pitfalls of high-pass filtering for detecting epileptic oscillations: a technical note on "false" ripples. Clin Neurophysiol 121 (3), 301–310. https://doi.org/10.1016/j.clinph.2009.10.019.

Blümcke, I., Thom, M., Aronica, E., Armstrong, D.D., Bartolomei, F., Bernasconi, A., et al., 2013. International consensus classification of hippocampal sclerosis in temporal lobe epilepsy: a task force report from the ILAE commission on diagnostic methods. Epilepsia 54 (7), 1315–1329. https://doi.org/10.1111/epi.12220.

Bragin, A., Engel Jr, J., Wilson, C.L., Fried, I., Buzsáki, G., 1999. High-frequency oscillations in human brain. Hippocampus 9 (2), 137–142. https://doi.org/10.1002/(SICI)1098-1063(1999)9:2<137::AID-HIPO5>3.0.CO;2-0.

Bratu, F., Makhalova, J., Garnier, E., Villalon, S.M., Jegou, A., Bonini, F., et al., 2024. Permutation entropy-derived parameters to estimate the epileptogenic zone network. Epilepsia 65 (2), 389–401. https://doi.org/10.1111/epi.17849.

Canolty RT, Edwards E, Dalal SS, Soltani M, Nagarajan SS, Kirsch HE, et al. High gamma power is phase-locked to theta oscillations in human neocortex. Science 2006;313 (5793):1626-8. doi: 10.1126/science:1128115.

Colombet, B., Woodman, M., Badier, J.M., Bénar, C.G., 2015. AnyWave: A cross-platform and modular software for visualizing and processing electrophysiological signals. J Neurosci Methods 242, 118–126. https://doi.org/10.1016/j.jneumeth.2015.01.017.

Dellavale, D., Urdapilleta, E., Cámpora, N., Velarde, O.M., Kochen, S., Mato, G., 2020. Two types of ictal phase-amplitude couplings in epilepsy patients revealed by spectral harmonicity of intracerebral EEG recordings. Clin Neurophysiol 131 (8), 1866–1885. https://doi.org/10.1016/j.clinph.2020.04.160.

Edakawa, K., Yanagisawa, T., Kishima, H., Fukuma, R., Oshino, S., Khoo, H.M., et al., 2016. Detection of epileptic seizures using phase-amplitude coupling in intracranial electroencephalography. Sci Rep 6 (1), 25422. https://doi.org/10.1038/srep25422.

Elahian, B., Lado, N.E., Mankin, E., Vangala, S., Misra, A., Moxon, K., et al., 2018. Low-voltage fast seizures in humans begin with increased interneuron firing. Ann Neurol 84 (4), 588–600. https://doi.org/10.1002/ana.25325.

Engel Jr., J., 1993. Update on surgical treatment of the epilepsies: summary of the second international palm desert conference on the surgical treatment of the epilepsies (1992). Neurology 43 (8), 1612–1617. https://doi.org/10.1212/wnl.43.8.1612.

Evangelista, E., Bénar, C., Bonini, F., Carron, R., Colombet, B., Régis, J., et al., 2015. Does the thalamo-cortical synchrony play a role in seizure termination? Front Neurol 6 (6), 192. https://doi.org/10.3389/fneur.2015.00192.

Frauscher, B., Bartolomei, F., Kobayashi, K., Cimbalnik, J., Klooster, M.A., Rampp, S., et al., 2017. High-frequency oscillations: The state of clinical research. Epilepsia 58 (8), 1316–1329. https://doi.org/10.1111/epi.13829.

Grinenko, O., Li, J., Mosher, J.C., Wang, I.Z., Bulacio, J.C., Gonzalez-Martinez, J., Nair, D., Najm, I., Leahy, R.M., Chauvel, P., 2018. A fingerprint of the epileptogenic zone in human epilepsies. Brain 141 (1), 117–131. https://doi.org/10.1093/brain/awx306. PMID: 29253102; PMCID: PMC5837527.

Hashimoto, H., Khoo, H.M., Yanagisawa, T., Tani, N., Oshino, S., Kishima, H., et al., 2021. Phase-amplitude coupling of ripple activities during seizure evolution with theta phase. Clin Neurophysiol 132 (6), 1243–1253. https://doi.org/10.1016/j.clinph.2021.03.007.

Ibrahim, G.M., Wong, S.M., Anderson, R.A., Singh-Cadieux, G., Akiyama, T., Ochi, A., et al., 2014. Dynamic modulation of epileptic high frequency oscillations by the phase of slower cortical rhythms. Exp Neurol 251, 30–38. https://doi.org/10.1016/j.expneurol.2013.10.019.

Iimura, Y., Jones, K., Takada, L., Shimizu, I., Koyama, M., Hattori, K., et al., 2018. Strong coupling between slow oscillations and wide fast ripples in children with epileptic spasms: investigation of modulation index and occurrence rate. Epilepsia 59 (3), 544–554. https://doi.org/10.1111/epi.13995.

Ikeda, A., Yazawa, S., Kunieda, T., Araki, K., Aoki, T., Hattori, H., Taki, W., Shibasaki, H., 1997. Scalp-recorded, ictal focal DC shift in a patient with tonic seizure. Epilepsia 38 (12), 1350–1354. https://doi.org/10.1111/j.1528-1157.1997.tb00074.x.

Isnard J, Taussig D, Bartolomei F, Bourdillon P, Catenoix H, Chassoux F, et al. French guidelines on stereoelectroencephalography (SEEG) 2018;48(1):51–3. doi: 10.1016/j.neucli.

Jacobs, J., Wu, J.Y., Perucca, P., Zelmann, R., Mader, M., Dubeau, F., et al., 2018. Removing high-frequency oscillations: a prospective multicenter study on seizure outcome. Neurology 91 (11), e1040–e1052. https://doi.org/10.1212/WNL.0000000000006158.

Jmail, N., Gavaret, M., Bartolomei, F., Bénar, C.G., 2017. Despiking SEEG signals reveals dynamics of gamma band preictal activity. Physiol Meas. 38 (2), N42–N56. https://doi.org/10.1088/1361-6579/38/2/N42 (Epub 2017 Jan 18 PMID: 28099166).

Jmail, N., Gavaret, M., Bartolomei, F., Chauvel, P., Badier, J.M., Bénar, C.G., 2016. Comparison of brain networks during interictal oscillations and spikes on magnetoencephalography and intracerebral EEG. Brain Topogr. 29 (5), 752–765. https://doi.org/10.1007/s10548-016-0501-7 (Epub 2016 Jun 22 PMID: 27334988).

Jurkiewicz, G.J., Hunt, M.J., Żygierewicz, J., 2021. Addressing pitfalls in phase-amplitude coupling analysis with an extended modulation index toolbox. Neuroinformatics 19 (2), 319–345. https://doi.org/10.1007/s12021-020-09487-3.

Kanda, Y., 2013. Investigation of the freely available easy-to-use software "EZR" for medical statistics. Bone Marrow Transplant 48 (3), 452–458. https://doi.org/10.1038/bmt.2012.244.

Köksal-Ersöz, E., Lazazzera, R., Yochum, M., Merlet, I., Makhalova, J., Mercadal, B., et al., 2022. Signal processing and computational modeling for interpretation of SEEG-recorded interictal epileptiform discharges in epileptogenic and non-epileptogenic zones. J Neural Eng 19 (5), 055005. https://doi.org/10.1088/1741-2552/ac8fb4.

Lagarde, S., Buzori, S., Trebuchon, A., Carron, R., Scavarda, D., Milh, M., et al., 2019. The repertoire of seizure onset patterns in human focal epilepsies: determinants and prognostic values. Epilepsia 60 (1), 85–95. https://doi.org/10.1111/epi.14604.

Li, C., Liu, S., Wang, Z., Yuan, G., 2023. Classifying epileptic phase-amplitude coupling in SEEG using complex-valued convolutional neural network. Front Physiol 13, 1085530. https://doi.org/10.3389/fphys.2022.1085530.

Li, P., Karmakar, C., Yearwood, J., Venkatesh, S., Palaniswami, M., Liu, C., 2018. Detection of epileptic seizure based on entropy analysis of short-term EEG. PLoS One 13 (3), e0193691. https://doi.org/10.1371/journal.pone.0193691.

López-Madrona, V.J., Pérez-Montoyo, E., Álvarez-Salvado, E., Moratal, D., Herreras, O., Pereda, E., Mirasso, C.R., Canals, S., 2020. Different theta frameworks coexist in the rat hippocampus and are coordinated during memory-guided and novelty tasks. Elife 20 (9), e57313. https://doi.org/10.7554/eLife.57313. PMID: 32687054; PMCID: PMC7413668.

Louis, D.N., Perry, A., Reifenberger, G., von Deimling, A., Figarella-Branger, D., Cavenee, W.K., Ohgaki, H., Wiestler, O.D., Kleihues, P., Ellison, D.W., 2016. The 2016 World Health Organization classification of tumors of the central nervous system: a summary. Acta Neuropathol 131 (6), 803–820. https://doi.org/10.1007/s00401-016-1545-1.

Madhu, N., Ranta, R., Maillard, L., Koessler, L., 2012. A unified treatment of the reference estimation problem in depth EEG recordings. Med Biol Eng Comput. 50 (10), 1003–1015. https://doi.org/10.1007/s11517-012-0946-0 (Epub 2012 Sep 16 PMID: 22983680).

Medina Villalon, S., Makhalova, J., López-Madrona, V.J., Garnier, E., Badier, J.M., Bartolomei, F., Bénar, C.G., 2024. Combining independent component analysis and source localization for improving spatial sampling of stereoelectroencephalography in epilepsy. Sci Rep. 14 (1), 4071. https://doi.org/10.1038/s41598-024-54359-4. PMID: 38374380; PMCID: PMC10876572.

Miyakoshi, M., Delorme, A., Mullen, T., Kojima, K., Makeig, S., Asano, E., 2013. Automated detection of cross-frequency coupling in the electrocorticogram for clinical inspection. Annu Int Conf IEEE Eng Med Biol Soc 3282–3285. https://doi.org/10.1109/EMBC.2013.6610242.

Motoi, H., Miyakoshi, M., Abel, T.J., Jeong, J.W., Nakai, Y., Sugiura, A., et al., 2018. Phase-amplitude coupling between interictal high-frequency activity and slow waves in epilepsy surgery. Epilepsia 59 (10), 1954–1965. https://doi.org/10.1111/epi.14544.

Nariai, H., Matsuzaki, N., Juhász, C., Nagasawa, T., Sood, S., Chugani, H.T., et al., 2011. Ictal high-frequency oscillations at 80–200 Hz coupled with delta phase in epileptic spasms. Epilepsia 52 (10), e130–e134. https://doi.org/10.1111/j.1528-1167.2011.03263.x.

Nonoda, Y., Miyakoshi, M., Ojeda, A., Makeig, S., Juhász, C., Sood, S., et al., 2016. Interictal high-frequency oscillations generated by seizure onset and eloquent areas may be differentially coupled with different slow waves. Clin Neurophysiol 127 (6), 2489–2499. https://doi.org/10.1016/j.clinph.2016.03.022.

Özkurt, T.E., Schnitzler, A., 2011. A critical note on the definition of phase-amplitude cross-frequency coupling. J Neurosci Methods 201 (2), 438–443. https://doi.org/10.1016/j.jneumeth.2011.08.014.

Roehri, N., Bartolomei, F., 2019. Are high-frequency oscillations better biomarkers of the epileptogenic zone than spikes? Curr Opin Neurol 32 (2), 213–219. https://doi.org/10.1097/WCO.0000000000000663.

Roehri, N., Pizzo, F., Lagarde, S., Lambert, I., Nica, A., McGonigal, A., Giusiano, B., Bartolomei, F., Bénar, C.G., 2018. High-frequency oscillations are not better biomarkers of epileptogenic tissues than spikes. Ann Neurol. 83 (1), 84–97. https://doi.org/10.1002/ana.25124 (PMID: 29244226).

Shokooh, L.A., Toffa, D.H., Pouliot, P., Lesage, F., Nguyen, D.K., 2021. Intracranial EEG seizure onset and termination patterns and their association. Epilepsy Res 176, 106739. https://doi.org/10.1016/j.eplepsyres.2021.106739.

Thomas, J., Kahane, P., Abdallah, C., Avigdor, T., Zweiphenning, W.J.E.M., Chabardes, S., Jaber, K., Latreille, V., Minotti, L., Hall, J., Dubeau, F., Gotman, J., Frauscher, B., 2023. A subpopulation of spikes predicts successful epilepsy surgery outcome. Ann Neurol. 93 (3), 522–535. https://doi.org/10.1002/ana.26548 (Epub 2022 Dec 10 PMID: 36373178).

Thompson, S.A., Krishnan, B., Gonzalez-Martinez, J., Bulacio, J., Jehi, L., Mosher, J., Alexopoulos, A., Burgess, R.C., 2016. Ictal infraslow activity in stereoelectroencephalography: Beyond the "DC shift". Clin Neurophysiol. 127 (1), 117–128. https://doi.org/10.1016/j.clinph.2015.03.020 (Epub 2015 Apr 11 PMID: 25920940).

Ueda, T., Iimura, Y., Mitsuhashi, T., Suzuki, H., Miao, Y., Nishioka, K., et al., 2023. Chronological changes in phase-amplitude coupling during epileptic seizures in patients with temporal lobe epilepsy. Clin Neurophysiol 148, 44–51. https://doi.org/10.1016/j.clinph.2023.01.014.

Urrestarazu, E., Jirsch, J.D., LeVan, P., Hall, J., Avoli, M., Dubeau, F., 2006. High-frequency intracerebral EEG activity (100–500 Hz) following interictal spikes. Epilepsia 47 (9), 1465–1476. https://doi.org/10.1111/j.1528-1167.2006.00618.x.

Weiss, S.A., Banks, G.P., McKhann, G.M., Goodman, R.R., Emerson, R.G., Trevelyan, A.J., et al., 2013. Ictal high-frequency oscillations distinguish two types of seizure territories in humans. Brain 136 (12), 3796–3808. https://doi.org/10.1093/brain/awt276.

Wendling, F., Bartolomei, F., Bellanger, J.J., Bourien, J., Chauvel, P., 2003. Epileptic fast intracerebral EEG activity: evidence for spatial decorrelation at seizure onset. Brain 126 (6), 1449–1459. https://doi.org/10.1093/brain/awg144.